ISSN (Print) 1226-1750
ISSN (Online) 2233-6656
Journal of Magnetics 25(3), 434-439 (2020) https://doi.org/10.4283/JMAG.2020.25.3.434

Novel Time-Domain Parameters for Detection and Classification of Flaws Using Pulsed Eddy Current Technique

K. Sambasiva Rao[1], T. V. Beatriceveena[2], C. S. Angani[3], and Lucky Agarwal[4]*

[1]*Department of Electronics and Communication Engineering, Madanapalle Institute of Technology & Science, Madanapalle-517325, India*
[2]*Homi Bhabha National Institute, Anushakti Nagar, Mumbai-400094, India*
[3]*Department of Electronics and Physics, GIS, GITAM Deemed to be University, Visakhapatnam-530045, India*
[4]*School of Electronics Engineering, Vellore Institute of Technology, Chennai-600127, India*

(Received 11 June 2020, Received in final form 23 September 2020, Accepted 24 September 2020)

Pulsed eddy current (PEC) testing is an electromagnetic nondestructive evaluation (NDE) technique which is used for detection and classification of flaws. This paper presents an approach for the extraction of novel time-domain flaw parameters viz. amplitude ratio (V_1/V_0) and time constant (τ) for detection and classification of different flaws. Experiments are carried out on stainless steel (SS-316) plate with artificial EDM notches whose width (1.0 mm & 3.0 mm) and depth (1.0 mm to 6.0 mm) varied. The proposed approach can classify both surface and sub-surface flaws in an 8.0 mm thick SS plate. The advantage of the proposed approach is that it doesn't require a reference signal subtraction or signal processing methodologies for the detection and classification of flaws.

Keywords : pulsed eddy current, amplitude ratio, time constant, flaws and classification

1. Introduction

Nondestructive testing (NDT) is carried out to materials and parts in ways that do not adversely affect their reusability [1]. Detection and classification of flaws with respect to type and size is essential for ensuring quality and structural integrity. This is accomplished by using NDE techniques [2, 3].

Among various NDE techniques, the eddy current technique is widely used for the detection of the surface [4], near-surface [5] flaws and measurement of coating thickness in electrically conductive materials [6, 7]. Conventional eddy current testing uses one or more frequencies for excitation to cover limited the depth of interrogation [8, 9].

In contrast to other electromagnetic techniques, such as conventional eddy current testing (ECT), multiple frequency eddy current (MFEC), and swept frequency eddy current (SFEC), the pulsed eddy current (PEC) technique uses a pulse [10-12] to excite the coil for interrogation of flaws at multiple depths. Since the pulse consists of a broad frequency spectrum, the reflected signal contains more information about flaws at different depths at once [13]. PEC has many advantages; including a wide spectrum of frequency components, fast detection speed, and broad application prospects [14]. Physically, the pulse is broadened and delayed as it travels deeper into the highly dispersive material and flaws or other anomalies close to the surface affect the eddy current response earlier than the deeper flaws [15]. Pulsed eddy current (PEC) testing is demonstrated capable of measuring the thickness and conductivity of metals [16, 17]. It is particularly devised and developed for the detection of sub-surface flaws, imaging and flaw characterization [18, 19].

Characterization of flaws in PEC testing is three-step processes: 1. flaw detection, 2. classification and 3. quantification. Flaw detection is the first stage where a feature is usually used to detect whether the sample being tested has a flaw or not. If a flaw is detected then the second stage is flaw classification. Here, the flaws are classified as surface and subsurface. Subsequently, sizing or quantification of flaws is performed to gain information about the severity of the detected flaw [20]. Among the three steps, defect classification plays a major role, as it is

*Corresponding author: Tel: +91-8004347806
Fax: +918571-280433, e-mail: rel1408@mnnit.ac.in

the foundation of accurate defect sizing at the later stages.

In the recent works about flaw classification, Chen *et al.* used new time-domain parameters such as RS, DS, TPDER, TTDER, RCUR and DCUR from the PEC signals for the classification of thickness, surface and sub-surface flaws [21]. Yang *et al.* proposed a comparative study for flaw classification based on ICA (independent component analysis) and PCA (principal component analysis) model. It is observed that the ICA model has shown improved flaw classification [22]. Zhang *et al.* proposed time and frequency domain feature fusion for flaw Classification. A new parameter called SCOVIF (sum of instantaneous frequency covariance) has been extracted and used for classification of thickness variation, surface and sub-surface flaws [23]. Sophian *et al.* introduced the application of PCA to extract the features for classification of surface, sub-surface flaws and wall loss [24]. From the literature, it is observed that classification has been carried out for thickness variation, surface and sub-surface flaws.

Detection and classification of surface and sub-surface flaws at a deeper location has been carried by using time-domain parameter in aircraft, nuclear, oil and gas industries. Some of the authors have carried out research on the effect of flaw width on the detection of flaws [25-26]. He *et al.* used the amplitude parameter for the detection of flaws in the aircraft reverted structures at variable flaw widths. It is found from the results that the amplitude parameter increases with an increase in flaw width [25]. He *et al.* identified peak amplitude and Rise time parameters for detection and classification of surface and sub-surface flaws for different width at 1.0 mm below the surface in an aluminum sample [26].

However, these parameters have been influenced by depth as well as the width of the flaw. For accurate classification and quantification of flaws, a systematic study on the effect of the flaw depth and width is necessary. Hence, the present work focuses on the detection and classification of flaws with varying width and depth at a deeper location.

The aim of this paper is to classify both surface and sub-surface flaws with varying width and depth beyond 3.0 mm by new time-domain parameters (Amplitude ratio, V_1/V_0 and Time constant, τ) by applying a modified inductor equation to the PEC signals. The rest of the paper is organized as follows. Section 2 explains the proposed approach and extraction of novel parameters for flaw detection and classification. Section 3 discusses the design and development of a high sensitive PEC instrument and fabrication of Electrical Discharge Machining (EDM) notches in the SS plate. Section 4 explains the experimental results and classification. Finally, conclusion and future work are outlined in Section 5.

2. Extraction of Novel Flaw Parameters

PEC data analysis is carried out in the time-domain by subtracting a reference signal from the flaw. The reference signal is obtained by keeping the probe over the flaw-free region. Further, the flaw parameters are extracted from the subtracted signals which are used for detection, classification and quantification of flaws. The commonly used parameters in the PEC technique are the peak amplitude (V_p) time-to-peak (T_p) and rising point (t_r) [27, 13]. Presence of noise in the reference signal affects the PEC parameters which cause inaccuracy in the detection of flaws [28]. The averaging method and wavelet transform based de-noising method is used to reduce noise in the measured signals which increases the computational burden [25].

In this paper, the authors proposed the extraction of novel time-domain parameters viz. amplitude ratio (V_1/V_0) and time constant (τ) without subtraction, averaging and signal processing of GMR signals and by fitting the modified inductor current equation to them as given in the Eq. (1). The physical meaning of the equation and extraction of flaw procedure has been given author's previous paper [29]. Figure 1 shows the block diagram of the proposed approach for the extraction of flaw parameters and classification of flaws. DC offset present in the PEC measurements. To eliminate offset, base correction has been carried out by subtracting the average of the first ten amplitude values from the GMR signals. Further, these signals have been fitted to the equation (1) to extract the flaw parameters:

$$V = (V_0 - V_1 \times \exp(-t/\tau)) \quad (1)$$

where V is the sensor output voltage, volts. V_0 and V_1 are the amplitude parameters which vary with volume loss of

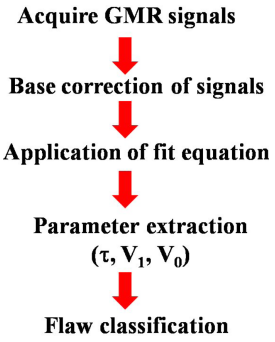

Fig. 1. (Color online) Proposed approach for flaw classification.

the flaws and τ is the time constant which varies on the dimension and location of the flaw.

3. Experimentation

The PEC experimental setup consists of an excitation unit, a PEC probe, a receiver unit, an analog to digital (A/D) converter and a personal computer. The PEC probe is a send-receive probe consisting of an excitation coil and a GMR sensor for pickup. The excitation coil was excited with a peak current of 0.6 A with a pulse width of 4.0 ms on the duration and a 100 Hz pulse repetition rate (PRR). The excitation coil having an inner diameter and an outer diameter of 8.0 & 20.0 mm with a height of 12.0 mm respectively. The number of turns used for the fabrication of the excitation coil is 250 with a SWG (standard wire gauge) of 32. The excitation unit is capable of producing high current variable voltage rectangular pulses to drive the excitation coil. The pickup sensor (GMR) is kept at the center of an excitation coil whose cylindrical axis is perpendicular to the test plate. Typical, GMR sensor output voltage is in the order of mV's, and this is usually dominated by external noise that degrades the signal-to-noise (SNR). In order to selectively amplify the GMR signals, a receiver unit has been designed along with a variable cut-off frequency low pass filter (LPF) circuit. The experimental setup of the developed PEC instrument as shown in Fig. 2.

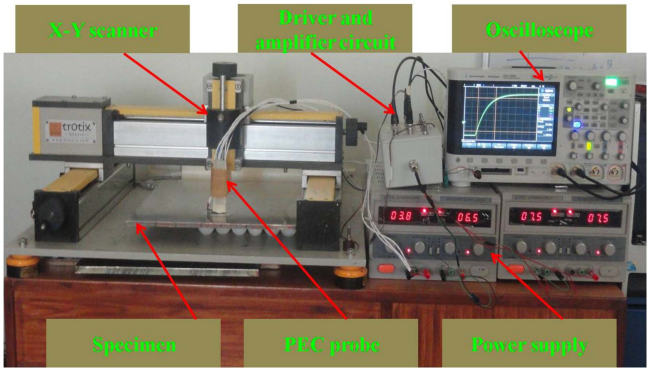

Fig. 2. (Color online) PEC experimental setup.

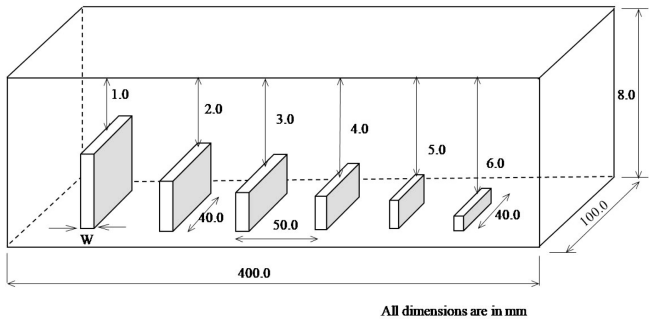

Fig. 3. (Color online) 3D view of the test sample whose flaw width is varied as 1.0 and 3.0 mm and depth varied from 1.0 to 6.0 mm.

To evaluate the performance of the proposed PEC system and approach, experiments are carried out on the artificial EDM notches in an 8.0 mm thick SS plate. Here, the flaws with two different widths (w = 1.0 and 3.0 mm) and varying depths from 1.0 to 6.0 mm are selected for the experimentation. The dimensional details of the specimen and flaws are shown in Fig. 3. Overall, 24 different dimensions of the flaws are selected for the experimentation, out of which 12 are surface flaws and the remaining are sub-surface flaws.

The PEC probe is interfaced to an X-Y scanner for automated scanning of the test specimen. The scanner is controlled using a NI PCI-7330 motion control card and LabVIEW software. The PEC probe is scanned over both

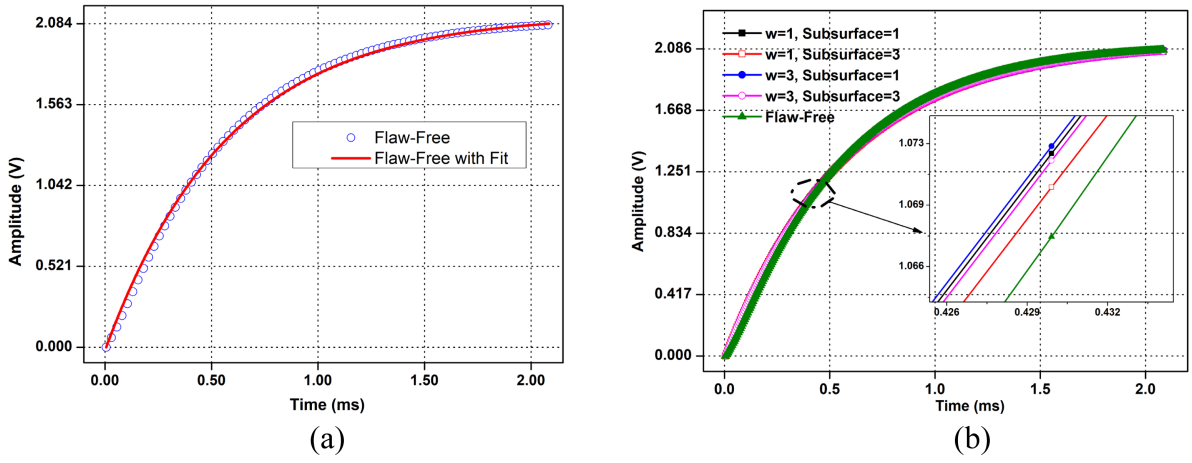

Fig. 4. (Color online) (a) Flaw free signal with the Fit and (b) Fit signals for the two different widths at subsurface location from 1.0 and 3.0 mm along with flaw-free signal.

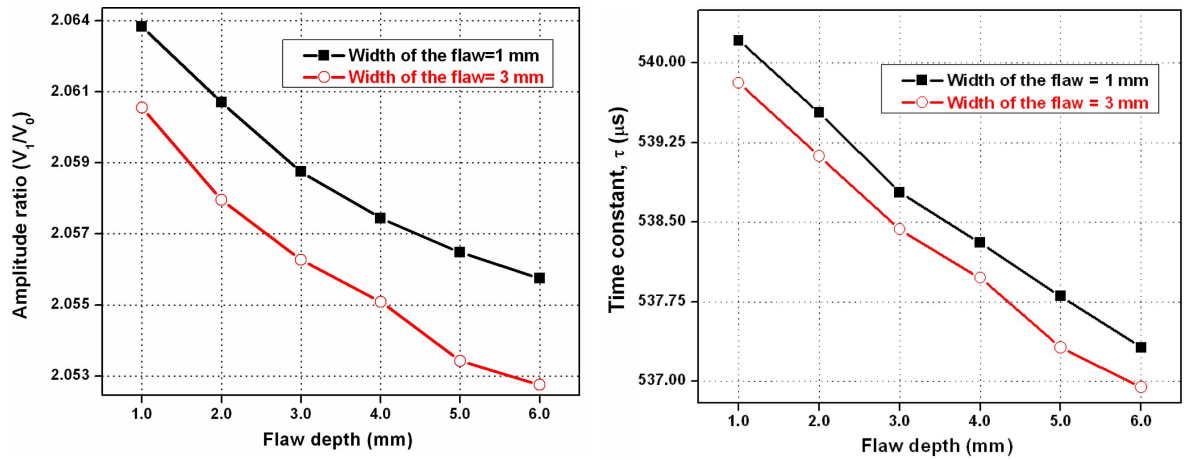

Fig. 5. (Color online) PEC novel parameters for surface flaws (a) amplitude parameter and (b) time constant.

surface and subsurface flaws in an 8.0 mm thick SS plate and flaw parameters are extracted from the response signal.

4. Results and Discussions

4.1. Detection of surface flaws

The time-domain flaw-free signal is shown with an open circle and the fit signal (to Eq. 1) is shown with a solid line in Fig. 4(a). It can be seen from the Fig. 4(a) that the fit signal is as close to the original signal with a R-value of 0.9998. The time-domain flaw signals typically considered as sub-surface flaws of 1.0 and 3.0 mm depth for two different widths along with flaw-free signals as shown in Fig. 4(b). As can be seen from the inset of Fig. 4(b) that the flaw-free signal is delayed more followed by the 1.0 mm and then 3.0 mm width signals.

For detection of surface flaws, the probe is scanned over the flaws of 1.0, 3.0 mm width and depths are varied from 1.0 to 6.0 mm. Figure 5(a) shows the variation of amplitude parameter (V_1/V_0) with respect to surface flaw depth (1.0 to 6.0 mm) for two different flaw widths (1.0 and 3.0 mm). The parameter decreases with increase in surface flaw depth. As discussed in Section 2.0, V_1 measures the resultant magnetic field due to induced eddy current in the plate. Increase in the depth of the surface flaw infers more of volume loss and less of the induced eddy current and hence, decrease in V_1 value. Similarly the amplitude parameter value is higher for flaw width of 1.0 mm than 3.0 mm. This is due to at a constant flaw depth and length, flaw width of 1.0 mm having less volume loss compared to width of 3.0 mm. Figure 5(b)

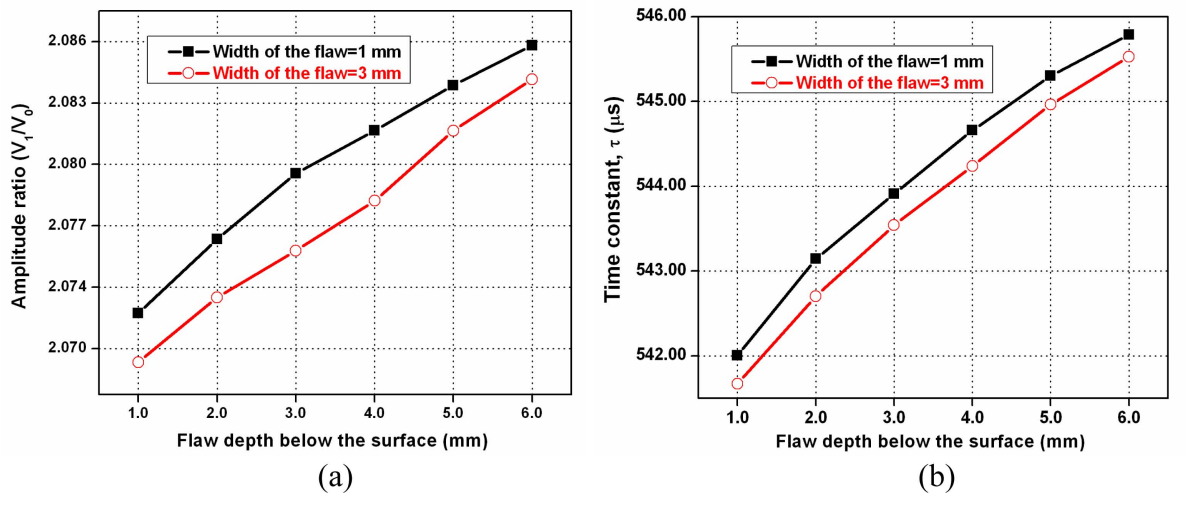

Fig. 6. (Color online) PEC novel parameters for sub-surface flaws (a) amplitude parameter and (b) time constant.

shows the variation of time constant (τ) parameter with respect to surface flaw depth for two different flaw widths. As can be observed, the time constant decreases with increase in surface flaw depth. This is attributed to higher the volume loss of the flaw results increase in net resistance seen by the probe which decreases the L/R ratio and hence, the time constant of the PEC signal.

4.2. Detection of sub-surface flaws

For sub-surface flaw detection, the probe is placed over the other side of the plate where the flaws are opened to the surface. Figure 6(a) shows the variation of amplitude ratio (V_1/V_0) parameter with respect to flaw location below the surface (1.0 to 6.0 mm) for two different flaw widths (1.0 and 3.0 mm). It increases with an increase in flaw location below the surface. This is due to the fact that as an increase in flaw location below the surface, the lesser the amount of the volume loss and hence more of the induced eddy currents in the test plate which results in increase in V_1 value. However, the value of V_1/V_0 is higher for the flaw width of 1.0 mm than 3.0 mm. It infers that, at a constant flaw depth and length, flaw width of 1.0 mm having less volume loss compared to a width of 3.0 mm. Therefore, the higher the value of V_1/V_0 for the flaws whose width is 1.0 mm compared with 3.0 mm.

Figure 6(b) shows the variation of time constant (τ) parameter with respect to the flaw location below the surface for two different flaw widths. As can be seen that the time constant increases with an increase in flaw location below the surface and it is higher for 1.0 mm flaw width. This attributed to, as the depth of the sub-surface flaw increases (flaw is away from the probe) causes a decrease in net resistance seen by the probe which results, increases in L/R ratio and hence, the time constant.

4.3. Classification of flaws

The previous sections discuss the detection of different types of flaws (both surface and sub-surface) using new time-domain parameters (V_1/V_0 and τ). This section explains the 2-D classification of different types of flaws present in the SS plate. To make a reliable detection and classification of flaws, at least two parameters are required. Figure 7 shows the 2-D classification results using the proposed parameters i.e. amplitude ratio (V_1/V_0) and the time constant (τ).

It can be observed from Fig. 7 (a) & (b) that the amplitude ratio (V_1/V_0) and time constant (τ) parameters from the proposed approach are effectively classified the surface and sub-surface flaws for two different flaw widths (1.0 and 3.0 mm) separately. Fig. 7(c) shows the

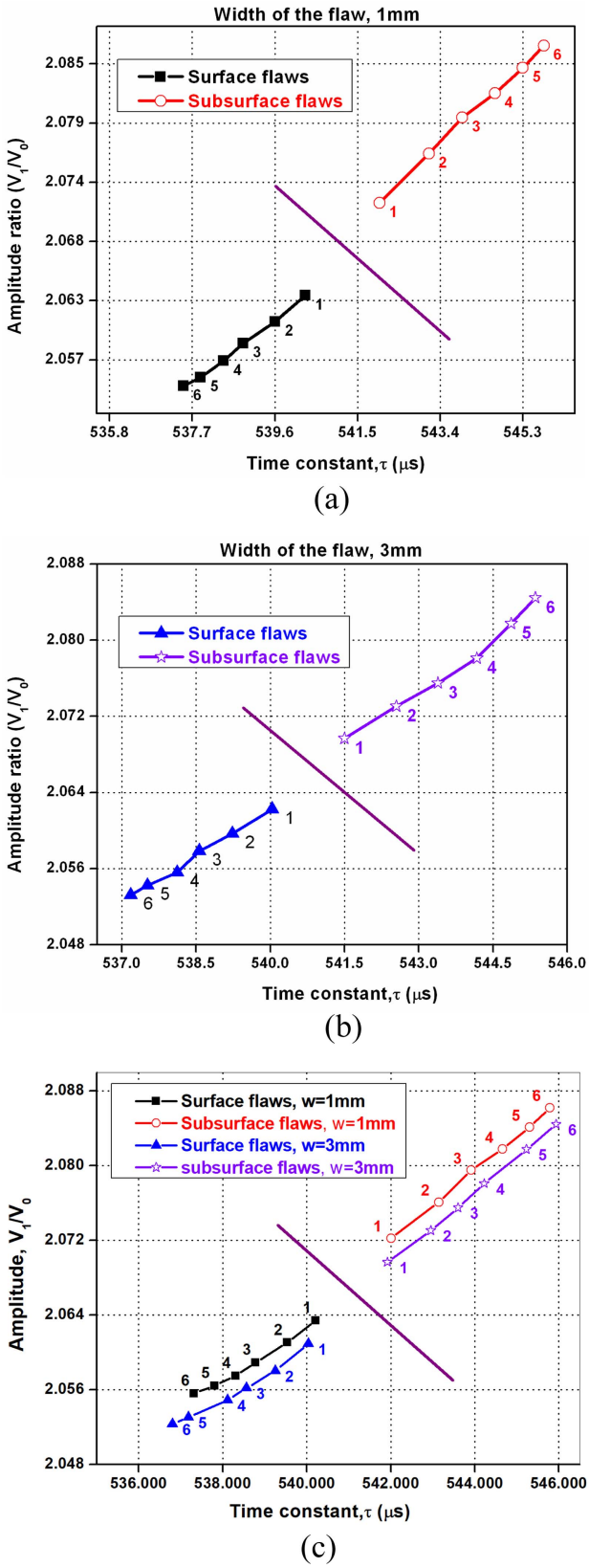

Fig. 7. (Color online) Classification of surface and sub-surface flaws for (a) flaw width = 1.0 mm (b) flaw width = 3.0 mm and (c) flaw widths = 1.0 and 3.0 mm.

combined 2-D classification of flaw widths 1.0 and 3.0 mm for different flaw depths (1.0 to 6.0 mm). It shows that the potential of the proposed approach is able to classify both surface and sub-surface flaw depths at different widths. The proposed approach doesn't require either reference signal subtraction to extract the flaw parameter or signal processing methods for the detection and classification of flaws. However, the classification distinction between 1.0 mm and 3.0 mm width of flaws is less. Further, works are in progress to improve the classification of flaw widths 1.0 mm and 3.0 mm by the application of artificial intelligence, machine learning and deep learning techniques.

5. Conclusions

Novel PEC parameters have been proposed in the time-domain for detection and classification of flaws. The parameters have been obtained by fitting the GMR response pulses from the flaws with the modified inductor current equation. The flaw parameters viz. amplitude ratio (V_1/V_0) and time constant (τ) have been extracted from the fit process. The flaw parameters are varying systematically with respect to width, depth and volume loss of the flaws. For surface flaws, both the parameters decrease with an increase in volume loss of the flaws whereas for sub-surface flaws, increase with a decrease in volume loss. The advantage of the proposed approach is that it doesn't require either a reference signal subtraction or signal processing for feature extraction and classification. The proposed parameters are able to classify (24-different types of flaw dimensions) both surface and sub-surface flaws effectively whose depth varying from 1.0 to 6.0 mm and width 1.0 & 3.0 mm effectively in a 8.0 mm thick SS plate. Therefore, these parameters can be used for NDE of other metallic materials and components. Further, works are in progress for the detection and classification of flaws in the multilayer aircraft structures with a high resolution using machine learning and deep learning concepts.

References

[1] H. Libby, Introduction to Electromagnetic Nondestructive Test Methods.: (New York: Wiley-Interscience), (1971).
[2] B. P. C. Rao, Practical Eddy Current Testing.: Alpha Science Int'l Ltd., (2007).
[3] M. Aoyagi, T. Hiraguri, and T. Ueno, Insight-Non-Destructive Testing and Condition Monitoring **57**, 269 (2015).
[4] Amine Asadi, Majid Abbasi, and Maryam Shamgholi, Res. Nondestr. Eval. **29**, 38 (2018).
[5] Yong Li, Bei Yan, Haoqing Jing, Yi Wang, Jinhua Hu, and Zhenmao Chen, Res. Nondestr. Eval. **30**, 287 (2019).
[6] Mengbao Fan, Qi Wang, Binghua Cao, Bo Ye, Ali Imam Sunny, and Guiyun Tian, Sensors **16**, 1 (2016).
[7] Li Yong, Zhenmao Chen, Ying Mao, and Qi Yong, NDT&E. Int. **50**, 29 (2012).
[8] R. A. Smith, D. Edgar, J. Skramstad, and J. Buckley, Insight-Non-Destructive Testing and Condition Monitoring **46**, 88 (2004).
[9] A. Habibalahi and M. S. Safizadeh, Insight-Non-Destructive Testing and Condition Monitoring **55**, 492 (2013).
[10] M. S. Safizadeh, B. A. Lepine, D. S. Forsyth, and A. Fahr, J. Nondestr. Eval. **20**, 73 (2001).
[11] Gui Yun Tian and Ali Sophian, NDT&E. Int. **38**, 319 (2005).
[12] Mingjiang Shi, Honghui Zhao, Zhiqiang Huang, and Lu Jiang, J. Magn. **23**, 142 (2018).
[13] Gui Yun Tian and Ali Sophian, NDT&E. Int. **38**, 77 (2005).
[14] Deqiang Zhou, Jun Wang, Jialong Wu, Ruizhen Yang, Hong Zhang, and Qiuju Zhang, Insight-Non-Destructive Testing and Condition Monitoring **58**, 87 (2016).
[15] S. Majidnia, J. Rudlin, and R. Nilavalan, Insight-Non-Destructive Testing and Condition Monitoring **56**, 560 (2014).
[16] Cheng-Chi Tai, J. H. Rose, and J. C. Moulder, Rev. sci. Instrum. **67**, 3965 (1996).
[17] Hung-Chi Yang, and Cheng-Chi Tai, Meas. Sci. Technol. **13**, 12 (2002).
[18] R. A. Smith and G. R. Hugo, 5th Joint NASA/FAA/DoD Aging Aircraft Conference., 2001.
[19] Gui Yun Tian, Ali Sophian, David Taylor, and John Rudlin, IEEE Sens. J. **5**, 90 (2005).
[20] G. Y. Tian, A. Sophian, D. Taylor, and J. Rudlin, IEE Proceedings-Science, Meas.Technol. **152**, 141 (2005).
[21] Tianlu Chen, Gui Yun Tian, Ali Sophian, and Pei Wen Que, NDT&E. Int. **41**, 467 (2008).
[22] Guang Yang, Gui Yun Tian, Pei Wen Que, and Tian Lu Chen, Res. Nondestr. Eval. **20**, 230 (2009).
[23] Qi Zhang, Tian-lu Chen, Guang Yang, and Li Liu, Res. Nondestr. Eval. **23**, 171, (2012).
[24] Ali Sophiani, Gui Yun Tian, David Taylor, and John Rudlin, NDT&E. Int. **36**, 37 (2003).
[25] Yunze He, Feilu Luo, Mengchun Pan, Feibing Weng, Xiangchao Hu, Junzhe Gao, and Bo Liu, NDT&E. Int. **43**, 176 (2010).
[26] Yunze He, Feilu Luo, Mengchun Pan, Xiangchao Hu, Junzhe Gao, and Bo Liu, Sens. Actuat.A-Phys. **157**, 26 (2010)
[27] V. Arjun, B. Sasi, B. Purna Chandra Rao, C. K. Mukhopadhyay, and T. Jayakumar, Sens. Actuat. A-Phys. **226**, 69 (2015).
[28] K. Samba Siva Rao, B. Purna Chandra Rao, and S. Thirunavukkarasu, IETE. Tech. Rev. **34**, 1 (2016).
[29] K. Sambasiva Rao, S. Mahadevan, B. Purna Chandra Rao, and S. Thirunavukkarasu, Measurement **128**, 516 (2018).